

INOTROPIC STIMULATION INDUCES CARDIAC DYSFUNCTION IN TRANSGENIC MICE EXPRESSING A TROPONIN T (I79N) MUTATION LINKED TO FAMILIAL HYPERTROPHIC CARDIOMYOPATHY

Björn C. Knollmann[&], Stephen A. Blatt[&], Kenneth Horton[¶], Fatima de Freitas[@], Todd Miller[@], Michael Bell[#], Philippe R. Housmans^{*}, Neil J. Weissman[¶], Martin Morad[%], and James D. Potter[@]

[&]Division of Clinical Pharmacology, Departments of Medicine and [%]Pharmacology, Georgetown University Medical Center, Washington, DC 20007; [¶]Cardiovascular Research Institute, Washington Hospital Center, Washington, DC 20010; ^{*}Department of Anesthesiology, Mayo Foundation, Rochester MN 55905; [@]Departments of Molecular and Cellular Pharmacology, and [#]Pathology, University of Miami School of Medicine, Miami, FL 33136

This work was supported by an American Heart Association fellowship: 9920387U (BCK); and National Institutes of Health Grants: 1) AR 45391 and 2R01 HL42325 (JDP); 2) R01 HL16152 (MM); 3) R01 GM36365 (PRH)

Corresponding address

Dr. James D. Potter
Professor and Chairman
Department of Molecular and Cellular Pharmacology
University of Miami School of Medicine
1600 N.W. 10th Ave.
Miami, FL 33136
305-243-5874
305-243-6233 (FAX)
jdpotter@miami.edu
<http://chroma.med.miami.edu/pharm/faculty/JPotter.html>

Running Title: **Cardiac dysfunction of TnT(I79N) transgenic mice**

Summary

The cardiac troponin T (TnT) I79N mutation has been linked to familial hypertrophic cardiomyopathy and a high incidence of sudden death, despite causing little or no cardiac hypertrophy. In skinned fibers, I79N increased myofilament calcium sensitivity (Miller *et al.*, JBC, in press). To further study the functional consequences of this mutation, we compared the cardiac performance of transgenic mice expressing either human TnT-I79N or human wild-type TnT. In isolated hearts, cardiac function was different depending on the Ca^{2+} concentration of the perfusate: Systolic function was significantly increased in Tg-I79N hearts at 0.5 and 1 mmol/l. At higher Ca^{2+} concentrations, systolic function was not different, but diastolic dysfunction became manifest as increased end-diastolic pressure and time to 90% relaxation. *In vivo* measurements by echocardiography and Doppler confirmed that baseline systolic function was significantly higher in Tg-I79N mice without evidence for diastolic dysfunction. Inotropic stimulation with isoproterenol resulted only in a modest contractile response, but caused significant mortality in Tg-I79N mice. Doppler studies ruled out aortic outflow obstruction and were consistent with increased chamber stiffness. We conclude that *in vivo*, the increased myofilament Ca^{2+} sensitivity due to the I79N mutation enhances baseline contractility, but leads to cardiac dysfunction during inotropic stimulation.

Introduction

Mutations in cardiac Troponin T (TnT) have been implicated in familial hypertrophic cardiomyopathy (FHC) (1-5). Individuals with cardiac TnT mutations appear to have a high incidence of sudden cardiac death at a young age, although heterozygote individuals have either little or no cardiac hypertrophy (1,3,4). At present, there is no clear understanding as to why TnT mutations in particular pose a high risk for sudden death, as opposed to, for example, mutations in the myosin heavy chain, which usually cause a much greater degree of cardiac hypertrophy. Sudden cardiac death of FHC patients is often caused by ventricular tachyarrhythmias (6), but its cause remains unknown for patients with TnT mutations. In fact, the clinical features of hypertrophic cardiomyopathy have been established mostly without knowledge of the genotype, and may not apply to patients carrying specific TnT mutations. Given the paucity of clinical information, a transgenic mouse model provides the opportunity to study the functional consequences of a TnT mutation in an *in vivo* system.

To investigate the mechanisms of how a TnT mutation alters cardiac function and lead to sudden cardiac death, we have generated transgenic mice expressing the human cardiac TnT-I79N mutant (Tg-I79N). Similar to humans carrying this mutation, Tg-I79N mice show no cardiac hypertrophy (7). We found a large increase in Ca^{2+} sensitivity of the skinned cardiac fibers from Tg-I79N mice compared to fibers from transgenic mice expressing human wild-type TnT (Tg-WT), but maximal developed force was significantly lower in cardiac fibers from Tg-I79N mice (7).

In this study we examined the effect of the I79N mutation on cardiac performance and electrophysiological properties of the whole heart, *in vitro* and *in vivo*. We found that the effect of the mutant protein was dependent on the inotropic state of the heart: Under baseline conditions, systolic function was higher in Tg-I79N mice, with little effect on diastolic function. However,

during inotropic stimulation with high extracellular Ca^{2+} or with isoproterenol, diastolic function was impaired, both in the isolated heart and *in vivo*. Based on these results, we conclude that the increased myofilament Ca^{2+} sensitivity due to the I79N mutation enhances baseline contractility, but leads to cardiac dysfunction during inotropic stimulation. In humans carrying the TnT-I79N mutation, this mechanism may contribute to excess mortality during exercise or in pathophysiological states with high levels of endogenous catecholamines, even in the absence of significant cardiac hypertrophy.

Experimental Procedures

Experimental Protocol

All studies were carried out according to NIH guidelines and approved by the institutional animal care and use committee. To examine the effect of the I79N mutation on cardiac performance and electrophysiology, we compared 3- to 4-month old mice: Transgenic mice expressing either human wild-type (Tg-WT, line 3) or mutant cardiac TnT (Tg-I79N, lines 8 and 9), and non-transgenic littermates (non-Tg). The generation and *in vitro* characterization of this transgenic model has been described (7). All three transgenic lines had high expression levels of the transgenic protein, with 70%, 52% and 34% replacement of endogenous mouse TnT (line 3, 8, and 9, respectively).

Isolated Perfused Heart Preparation

Mice were anesthetized with 20 ml/kg of 2% tribromoethanol (Avertin) via intraperitoneal (i.p.) injection. After a surgical level of anesthesia was confirmed, a thoracotomy performed, the heart removed and the animal killed by exsanguination. Hearts of 4 non-Tg, 5 Tg-WT and 5 Tg-I79N mice (line 9) were isolated and perfused in the Langendorff mode as described previously for mouse hearts (8). In brief, the chest was opened, the heart was rapidly excised and the aorta was cannulated. Retrograde perfusion via the aorta was carried out at a constant perfusion pressure of 68 mmHg at 37°C. The flow of Thebesian veins was drained via a thin polyethylene tube (PE-10) pierced through the apex of the left ventricle. Krebs-Henseleit buffer containing (mM): NaCl (118), KCl (4.7), CaCl₂ (2.5), MgSO₄ (1.2), Na-EDTA (0.5), NaHCO₃ (25), KH₂PO₄ (1.2), and glucose (11) was prepared at the time of the experiment. To maintain a constant heart rate, the atrioventricular node was ablated and the hearts were epicardially paced at 420 min⁻¹ via a bipolar Ag-AgCl contact electrode placed on the base of the right ventricle.

Hearts were allowed to equilibrate for 15 minutes before baseline left-ventricular pressures

recordings were obtained. To examine the effects of different inotropic states, the heart was then perfused with KH buffer containing free $[Ca^{2+}]$ of 0.5, 1, 2, 3, and 4 mM. Free $[Ca^{2+}]_o$ was calculated using Fabiato's program (9). Contractile measurements were obtained at the end of each 5 minutes at the respective $[Ca^{2+}]_o$. All perfusion buffers were equilibrated with 95% O₂ + 5% CO₂ for at least 1 hour prior to the experiment, yielding a pH of 7.4 .

Measurement of Isovolumic Cardiac Performance

A water-filled balloon custom-made of polyvinylchloride film was inserted through the mitral valve into the left ventricle via an incision in the left atrium as described (8). A 2.0-Fr microtip transducer (Millar, Inc, Texas) was guided through the polyethylene tube and positioned inside the balloon. The balloon was inflated to adjust the end-diastolic pressure (EDP) at 6-8 mmHg, and the balloon volume was held constant for the duration of the experiment. The left-ventricular pressure was digitized at 1000 samples/s with the use of a commercially available data acquisition system (PowerLab, ADInstruments, Inc.). The fast sampling rate coupled with the use of a pressure catheter with a flat frequency response up to 10 kHz allowed us to do the detailed kinetic analysis of the pressure recordings outlined below.

The following indices of cardiac performance were measured off-line using custom-built software (National Instruments, Inc.) and averaged from three consecutive beats at baseline and at the end of each Ca^{2+} concentration step: Left ventricular systolic pressure (SP), end-diastolic pressure (EDP), developed pressure (the difference between SP and EDP), the minimum and maximum values of the first derivative of left ventricular pressure (+dP/dt and -dP/dt), ratio of +dP/dt and -dP/dt, time to reach peak systolic pressure, time to reach peak +dP/dt, time from peak systolic pressure to reach 90% relaxation. To determine the time constant of isovolumic pressure decay, the

LV pressure curve was fitted from the time of minimum dP/dt to a level 5 mmHg above the EDP of the next beat using an monoexponential function as described (8).

Surface Electrocardiogram (ECG) and Systolic Blood Pressure Measurements

For the ECG measurements, mice were anesthetized either with ketamine (100 mg/kg) and xylazine (5 mg/kg), or with 20 ml/kg of 2% tribromoethanol (Avertin) via intraperitoneal (i.p.) injection. Mice were positioned prone in a shielded box, with all four extremities immersed in 3 M KCl filled wells to reduce skin resistance. The bottom of the shielded box was heated to 37°C using a circulating water bath to maintain a stable body temperature during the experiment. In order to accurately capture the ECG signals from mice, which have the high heart rates (500-600 beats) and a very short QRS duration, a custom-built ECG amplifier (Vibraspec, Bear Island, ME 04662) was used. This amplifier provided a high frequency response and large gain (1000 Hz and 10000 fold gain) and was used to record bipolar limb leads in standard fashion as described (10). Signals were digitized at 1 kHz using a National Instruments, Inc. data acquisition system with custom-built software. For each animal, PR and QRS intervals were measured from three consecutive beats in leads I and II and averaged. For QT and RR measurements, the recordings were signal-averaged over a 30 s time interval using the peak of the R-wave as the fiduciary point as described (11). This procedure reduced the effect of respiratory and motions artifacts on QT measurements. The RR interval was measured as the average over the 30 s interval, and the QT interval was measured in the lead with the longest and most prominent T-wave.

Systolic blood pressure and heart rate were measured in conscious and anesthetized mice using a commercially available, noninvasive computerized tail-cuff system (BP-2000, Visitech, Apex, NC).

Echocardiography and Doppler Measurements

Mice were anesthetized as for the ECG measurements and positioned supine on a heated surface (37°C) to maintain a stable body temperature during the experiment. Echocardiography and Doppler measurements were performed with a 1 cm gel standoff in a left-lateral position similar to the technique used by Hoit and colleagues (12). An Acuson Sequoia C256 system with a linear transducer in 13 MHz mode was used to obtain high-resolution two-dimensional (2-D) and M-mode measurements (17). A 2-D guided M-mode of the left ventricle (LV) was performed in short axis at the tip of the mitral leaflets and through the center of the LV cavity. The proper probe position was confirmed by rotating the probe 90-degree and obtaining 2D-guided long-axis M-mode measurements in the same animal. 2D-guided Doppler flow measurements of aortic outflow and mitral inflow were obtained. Mitral inflow velocities were recorded only after extensive scanning from multiple vantage points to insure that the maximal velocity was obtained. In most situations, this was an apical window that corresponds to an “off-axis” apical window (displaced toward the parasternal window). A limb-lead ECG was simultaneously recorded during echocardiography and stored both on computer, for off-line analysis, and on the echocardiogram videotape. The echo images were digitized from videotape and measurements performed using a digital image analysis package (Nova Microsonics/Kodak, Inc). Left ventricular (LV) end-systolic and end-diastolic internal diameters (LVIDS and LVIDD, respectively) and LV wall thickness were measured for each animal from the M-mode image. Aortic outflow velocity, aortic ejection time (ET), aortic acceleration time to peak outflow, early and late mitral inflow velocity (E-wave and A-wave, respectively), and E-wave deceleration time were measured from the Doppler recordings in standard fashion, and the E to A ratio calculated. To assess overall left-ventricular systolic performance, LV shortening fraction ($SF = (LVIDD - LVIDS) / LVIDD$) and heart-rate corrected velocity of circumferential fiber shortening ($VCFc = (SF)(RR^{0.5}) / ET$) were calculated.

Isoproterenol Application

Isoproterenol was given as a bolus intraperitoneal injection after stable baseline ECG and echocardiography recordings had been obtained (5-10 minutes). Mice were initially challenged with a dose of 1.5 mg/kg (high-dose) based on reports in the literature (12). After deaths occurred in the Tg-I79N group, we examined the effects of a lower dose (0.1 mg/kg), which was sufficient to produce a significant increase in heart rate in all 4 groups of mice. All ECG and echocardiographic assessments described above were repeated at 3-5 minutes after injection, when a significant increase in heart rate was present.

Mice Exercise Protocol

A swimming protocol described by Geisterfer-Lowrance *et.al* (13) was utilized to examine the effects of chronic aerobic exercise. Groups of 4 animals, 2 months old, representing the different lines, were exercised by swimming. Mice were adapted to the swimming program by beginning with 10 min sessions two times a day separated by 4 hours. These were incremented by 10 min per day until reaching 90 min per session. The program was completed in 4 weeks. During each session, they were monitored for inability to sustain the exercise and/or sudden death.

Autopsy and Histopathology of Tg-Mice

Every mouse that died during the isoproterenol challenge was autopsied to rule other causes of death such as hemorrhage. This is especially important because drugs were administered via intraperitoneal injection. One death (a non-Tg mouse) was indeed due to a hemorrhage from the right iliac artery close to the injection site. This animal was excluded from further analysis. We did not find any evidence for bleeding in any of the other deaths.

Three separate groups of mice (4 Non-Tg, 4 Tg-WT, Tg-I79N line 9), were specifically sacrificed to examine the heart morphology and histology. Two mice of each group had undergone

chronic exercise. After euthanasia, each mouse was autopsied with dissection of the heart. The heart was weighed and any gross abnormalities (chamber enlargement, mural thrombi, etc.) were recorded. The 10% buffered formalin fixed heart was sectioned along its transverse plane and embedded in paraffin. Microscopic sections were cut from the transected surface at 4-6 μm and stained with hematoxylin and eosin (H & E) for overall morphology and Mason's trichrome (MT) for collagen. The histologic slides were examined for the presence of asymmetric hypertrophy, fibrosis or myocyte disarray without knowledge of genotype, degree of exercise training, or *in vivo* test results.

Computer simulations

Force generation in Tg-WT and Tg-I79N myocardium was simulated by computer based on a modification of the model of Robertson et al. (14) and a two-state cross-bridge model (15) utilizing an exponential dependence of the TnC off-rate for Ca^{2+} (Ca^{2+} -specific site II) on force (16). These simulations have been extensively described in the accompanying paper (7).

Statistical Analysis

All experiments (Left-ventricular pressure, ECG and Echocardiography) were done in random sequence in respect to the genotype, and measurements were taken by a single observer who was blinded to the genotype. Differences between groups were assessed using a one-way analysis of variance (ANOVA). If statistically significant differences were found, individual groups were compared with Student's two-sided *t*-test without correction for multiple comparisons. Incidence rates were compared using Chi-square test statistic. Results were considered statistically significant if the *P*-value was less than 0.05. Unless otherwise indicated, results are expressed as means and standard error of the mean (SEM).

Results

Cardiac Performance of the Isolated Heart

Baseline measurements

To examine the functional consequences of the I79N mutation in the whole heart, we measured indices of cardiac performance in the isolated perfused, isovolumically-contracting heart. This experimental preparation permits exact control of the loading conditions, and has been used to examine both systolic and diastolic function in other murine models (8,17-19). Systolic function was assessed from systolic pressure, time to peak pressure, and maximum rate of pressure rise (+dP/dt). Diastolic function was assessed from the maximum rate of pressure decay (-dP/dt), and from time to 90% relaxation and the time constant of isovolumic relaxation. When hearts were paced at 420 min⁻¹ and end-diastolic pressure was set at 6-8 mmHg, systolic performance was not statistically different between Tg-I79N, Tg-WT, and non-Tg hearts (table 1). However, the initial rise of pressure was faster in Tg-I79N hearts (Fig. 1, arrow). Thus, time to maximum +dP/dt was significantly shorter in the Tg-I79N hearts (table 1). On the other hand, time to 90% relaxation and the relaxation time constant were significantly longer in the Tg-I79N hearts compared to both Tg-WT and non-Tg hearts (table 1). The pressure tracings of Fig. 1 illustrate the slower relaxation of the Tg-I79N hearts. The ratio of +dP/dt to -dP/dt, which can be used to assess diastolic function relative to systolic function (20), was significantly increased in Tg-I79N mice (table 1). Furthermore, the LV balloon volume at an end-diastolic pressure of 8 mmHg was lower in Tg-I79N mice (Tg-I79N: 13.0 ± 0.3 µl, Tg-WT: 15.1 ± 0.8 µl, p<0.05). Taken together, these results indicate that Tg-I79N hearts had significantly impaired diastolic function.

Force traces were simulated as would be observed during isometric twitch contractions of Tg-WT and Tg-I79N ventricular myocardium using variables (off-rate of Ca²⁺ from troponin C, and

cross-bridge dissociation constant) derived previously (7). Transgenic I79N myocardium relaxed slower than Tg-WT, which is consistent with the experimental observations in isovolumetrically beating heart.

Ca²⁺ dependence of cardiac performance

We also examined the changes in cardiac performance in response to changes in $[Ca^{2+}]_o$ (Fig. 2). At $[Ca^{2+}]_o$ of 0.5 and 1 mM, developed pressure was significantly higher in Tg-I79N than in Tg-WT hearts (Fig. 2A). At higher $[Ca^{2+}]_o$, however, developed pressure was not significantly different between the two groups. Thus, there was a leftward shift of the $[Ca^{2+}]_o$ – pressure relationship in Tg-I79N hearts. Indices of diastolic function demonstrated a different $[Ca^{2+}]_o$ dependence: At $[Ca^{2+}]_o$ of 0.5 and 1 mM, EDP was significantly lower in I79N hearts (Fig. 2B), while time to 90% relaxation was not significantly different from Tg-WT (Fig. 2C). At higher $[Ca^{2+}]_o$, EDP was significantly higher (Fig. 2B), and time to 90% relaxation was significantly longer in I79N hearts than in Tg-WT hearts (Fig. 2C). Therefore, I79N hearts demonstrate increased systolic performance at low $[Ca^{2+}]_o$, yet comparable to Tg-WT at a $[Ca^{2+}]_o$ of 2 mM or above. On the other hand, diastolic function is comparable to Tg-WT at low $[Ca^{2+}]_o$, but significantly impaired at high $[Ca^{2+}]_o$.

In vivo Cardiac Performance and Cardiac Electrophysiology of Tg mice

Baseline Echocardiography and Doppler measurements

Echocardiography and Doppler measurements have been used extensively to characterize the cardiac phenotype of transgenic mouse models (21). We measured cardiac dimensions, indices of systolic function and diastolic ventricular by 2D-guided M-mode (Fig. 3A) and Doppler (Fig. 3B). Table 2 summarizes the results. Indices of systolic contractile function (LV shortening fraction and VCFc) were significantly higher in both Tg-I79N lines compared to Tg-WT.

Evidence for increased contractility was also present on flow measurements by Doppler. Tg-I79N mice had a significantly shorter time to peak outflow velocity (Fig. 3B). Baseline diastolic filling parameters measured by Doppler (E-wave, A-wave, E-wave deceleration time, E/A ratio) were not statistically different between all 4 lines. Thus, unlike the isolated perfused heart, systolic function was increased in Tg-I79N mice, but diastolic function appeared to be normal. One reason for this apparent discrepancy may be related to the slow heart rates ($\sim 250 \text{ min}^{-1}$) induced by the ketamine/xylazine anesthesia. We therefore repeated the echocardiography and Doppler measurements using a different anesthetic, Avertin, which produces much less bradycardia. Since there were no large differences in the cardiac parameters between Tg-I79N lines 8 and 9, we compared Tg-I79N line 9 with Tg-WT mice and non-Tg mice. Heart rates indeed increased to a similar extent in all groups (table 2). Systolic function was significantly different between all three groups (LV shortening fraction: Tg-I79N $43 \pm 1.2 \%$, Tg-WT $27 \pm 1.2 \%$, non-Tg $33 \pm 1.2 \%$, $p < 0.00001$ by ANOVA). Interestingly, at these faster heart rates, the end-diastolic dimension was significantly smaller in Tg-I79N mice ($3.2 \pm 0.1 \text{ mm}$, $p < 0.0001$ against both WT and non-Tg) than in Tg-WT mice ($3.8 \pm 0.1 \text{ mm}$) or in non-Tg mice ($3.6 \pm 0.2 \text{ mm}$). Nevertheless, Doppler indices of diastolic filling were not significantly different. Unfortunately, the A-wave could only be measured in less than 30% of the examined animals.

To exclude the possibility that the differences in LV shortening fraction were merely due to a difference in afterload, we also measured the blood pressure in anesthetized mice (Avertin). Systolic blood pressure was not significantly different (Tg-I79N mice $95 \pm 4 \text{ mmHg}$, $n=10$, vs. Tg-WT $89 \pm 4 \text{ mmHg}$, $n=8$, $p=n.s.$). Taken together, these data demonstrate that anesthetized Tg-I79N mice have increased systolic cardiac performance *in vivo*. A likely explanation for the difference between the systolic function *in vivo* and in the isolated heart is the relatively low free $[\text{Ca}^{2+}]$ of

mouse blood: Average free $[Ca^{2+}]$ measured in 4 non-transgenic littermates after 15 minutes of ketamine/xylazine anesthesia was 1.26 ± 0.03 mM, which is significantly lower than the perfusate $[Ca^{2+}]$ for the baseline isolated heart recordings.

In another series of experiments, we examined whether the increased systolic function can be demonstrated in conscious Tg-I79N mice. Systolic blood pressure was not significantly different between Tg-I79N (112 ± 2 mmHg, n=32) and Tg-WT mice (114 ± 2 mmHg, n=23, p=n.s.). Heart rate, on the other hand, was significantly lower in Tg-I79N mice (521 b/min vs. 604 b/min, $p < 0.00001$). It remains to be determined whether the slow heart rate of Tg-I79N mice represents a vagal response to the increased cardiac contractility.

ECG measurements

Cardiac arrhythmias are a potential cause of sudden death. Limb-lead ECGs were recorded from anesthetized non-Tg, Tg-WT and Tg-I79N mice (Fig. 4A). The most significant finding was that Tg-I79N had a consistently prolonged PR interval representing the conduction time from the atria to the ventricle. The PR prolongation was independent of the anesthetic used (data not shown) and was more pronounced in chronically exercised mice (Fig. 4B). As shown in Fig. 4C, the degree of PR prolongation appeared to be related to the expression level of the mutant TnT protein: Line 8 with higher levels of Tg-I79N had more PR prolongation than line 9 with lower protein levels. Although PR prolongation is not a common ECG finding in FHC patients, left atrial enlargement is often observed. Left atrial hypertrophy in Tg-I79N mice was documented on autopsy. QRS duration and heart rate were not statistically different, but the QT-interval was significantly shorter in Tg-I79N mice (line 9: 43 ± 2.6 ms, n=8, line 8: 51 ± 6.0 ms, n=5, Tg-WT: 67 ± 4.5 ms, n=13, non-Tg: 67 ± 2.5 ms, n=13, $p < 0.05$ between groups). Arrhythmias were not observed in Tg-I79N mice at

baseline.

In vivo cardiac performance under inotropic stimulation

Based on the results from the isolated heart studies and the simulation studies, raising $[Ca^{2+}]_o$ predominantly affects diastolic function (Figs. 1 and 2). To test this hypothesis *in vivo*, we examined the effect of raising intracellular $[Ca^{2+}]$ via inotropic stimulation with isoproterenol, because it is difficult to raise plasma free $[Ca^{2+}]_o$ *in vivo* without causing significant toxicity. In order to detect abnormalities in diastolic function, Ketamine/xylazine anesthesia was used for echocardiography and Doppler studies, because, based on our experience from the baseline studies, it allowed better Doppler recordings of mitral inflow compared to Avertin anesthesia. When mice were injected with 1.5 mg/kg isoproterenol, several Tg-I79N mice died shortly after injection. Therefore, echocardiography and Doppler studies were performed with a lower dose of 0.1 mg/kg isoproterenol i.p. (table 2). Whereas isoproterenol produced a dramatic increase in contractility in non-TG and Tg-WT mice (LV shortening fraction increased by $26 \pm 3\%$ in Tg-WT, n=12), Tg-I79N mice showed a smaller inotropic response (LV shortening fraction increased only by $9 \pm 3\%$ and $8 \pm 3\%$ in line 9 and 8, n=7 and 6, $p < 0.01$ against WT). In fact, 4 out of 13 Tg-I79N mice, but none of the 12 Tg-WT mice, later developed global LV hypokinesia, and died. Doppler measurements demonstrated that this impaired inotropic response was not caused by an outflow obstruction, since both WT and I79N had similar aortic outflow velocities (see table 2). Impaired ventricular relaxation and increased diastolic chamber stiffness, as evidenced by the shorter E-wave deceleration time, loss of A-wave and increased E/A ratio on Doppler measurements in I79N mice (Fig. 5) likely contributed to the isoproterenol-induced cardiac dysfunction.

To further investigate the isoproterenol-induced deaths of TgI79N mice, we repeated the isoproterenol experiments with continuous ECG monitoring. At the lower dose (0.1mg/kg i.p.), 75%

of the examined Tg-I79N mice exhibited loss in R-wave amplitude, QRS widening and T-wave inversion, and 25% died (Fig. 6A). Heart rate peaked three minutes after injection of isoproterenol before significant ECG changes developed in the Tg-I79N mice. Despite a similar maximal heart rate in all four groups, the significant PR prolongation in the Tg-I79N mice was consistently observed (Tg-I79N line 8, n=5: 43 ± 3.2 ms, line 9, n=8: 44 ± 1.6 ms, Tg-WT, n=12: 35 ± 1.2 ms, non-Tg, n=13: 34 ± 0.8 ms, $p < 0.05$ Tg-79 vs. Tg-WT). QRS duration and QT interval were not statistically different between the four groups. At a higher dose of isoproterenol (1.5 mg/kg i.p.), all Tg-I79N mice exhibited loss in R-wave amplitude, QRS widening and T-wave inversion, and 75% of the animals died within 20 minutes of injection (Fig. 6B). Compared to the sustained acceleration in heart rate of Tg-WT mice, the same isoproterenol injection resulted only in a very transient increase in heart rate in Tg-I79N mice, followed by progressive conduction blocks and eventually death (Fig. 7). The insets in Fig. 7 illustrate the profound changes in QRS morphology (progressive loss in R-wave amplitude, QRS widening and T-wave inversion) that developed after isoproterenol injection. Ventricular tachyarrhythmias were observed only in a few mice, and were never sustained more than a few seconds. Tg-I79N mice died with progressive conduction blocks present on ECG. Autopsy examination demonstrated dilated atria with pulmonary and hepatic congestion, and no evidence for bleeding. Taken together, these data indicate that the isoproterenol-induced deaths were not caused by ventricular tachyarrhythmias. It remains to be determined whether the bradyarrhythmias were the primary cause of the deaths, or whether they were a secondary phenomenon; e.g. as a result of pulmonary edema and respiratory failure, which developed because of the isoproterenol-induced cardiac dysfunction.

Effect of chronic exercise

Eight Tg-WT, 8 Tg-I79N and 8 non-Tg mice underwent 4 weeks of chronic swimming

exercise. Two deaths occurred, one each in the Tg-WT and the Tg-I79N group. No apparent difference in exercise tolerance were observed between the groups. Except for the increase in PR interval in Tg-I79N mice (Fig. 4B), there were no other ECG abnormalities or arrhythmias found on ECG studies obtained after the completion of the exercise program.

Histopathology of Tg-mice

Hearts of Tg-I79N were smaller than age and sex-matched Tg-WT and non-Tg mice, with a significantly decreased heart weight to body weight ratio, as already reported in the preceding article (7). However, we found evidence for left atrial hypertrophy (left atrial weight Tg-I79N, line 9: 10 ± 2 mg vs. Tg-WT: 5 ± 1 mg, $n=6$ each, $p=0.08$), which was significantly different when the values were corrected for the lower ventricular weight of Tg-I79N mice (left atrial weight/heart weight ratio Tg-I79N: 0.048 ± 0.009 vs. Tg-WT: 0.023 ± 0.003 , $n=6$ each, $p=0.025$). Histological examinations of hematoxylin and eosin (H+E) stained ventricular sections from non-Tg, Tg-WT (line 3) and Tg-I79N (line 9) revealed normal myocyte architecture and no major differences between the three lines (Fig. 8, upper panels). Tg-WT (line 3) and Tg-I79N (line 9) may have somewhat more nuclear pleomorphism (greater variation in the size and appearance of the nuclei) than the non-Tg mice. On trichrome (TRIC) stained sections, which stains muscle and red blood cells red and areas containing fibrosis or collagen blue, no differences between the three lines were observed. Chronic exercise had no effect on cardiac histology in either group.

Discussion

The major finding of this study is that significant alterations in cardiac contractile and electrical properties occur in transgenic mice carrying the TnT-I79N mutation. In the isolated heart, the effect of the I79N mutation on cardiac performance depended on the Ca^{2+} concentration of the perfusate: Systolic function was significantly increased in Tg-I79N hearts only at 0.5 and 1 mmol/l $[\text{Ca}^{2+}]_o$, with no difference in diastolic function. At higher $[\text{Ca}^{2+}]_o$, diastolic dysfunction became manifest as both an increase in end-diastolic pressure and in time to 90% relaxation (table 1 and Figs. 1 and 2). *In vivo* measurements with echocardiography and Doppler confirmed that, at baseline, systolic function was significantly higher in Tg-I79N mice without evidence for diastolic dysfunction (Table 2 and Fig. 3). However, inotropic stimulation with isoproterenol resulted only in a modest initial contractile response, but later caused significant mortality only in Tg-I79N mice (Figs. 6). Doppler studies ruled out aortic outflow obstruction and were consistent with impaired diastolic filling (table 2 and Fig. 5). Continuous ECG monitoring ruled out ventricular tachyarrhythmias as cause of death and showed changes in ECG morphology and bradyarrhythmias (Fig.7). Morphological and histological studies ruled out significant ventricular hypertrophy, fibrosis or myocyte disarray (Fig. 8). Our results are consistent with the hypothesis that the increased myofilament Ca^{2+} sensitivity due to the I79N mutation enhances baseline contractility, but leads to cardiac dysfunction under inotropic stimulation. This mechanism may contribute to excess mortality during exercise or other states with high levels of endogenous catecholamines, even in the absence of significant cardiac hypertrophy.

Cardiac Performance of Tg-I79N mice

In the isolated heart of I79N mice, systolic function was higher, and relaxation was impaired.

Although no data from humans or other transgenic models carrying the I79N mutation exist, similar findings have been reported in a mouse model expressing the FHC-linked TnT-R92Q mutation (17-19), whereas impaired systolic function has been reported in an independently created transgenic mouse model of the same mutations (22). Data presented here may provide explanation for the disparate results: At low $[Ca^{2+}]_O$, the positive inotropic effect of the leftward shift in Ca^{2+} -sensitivity of skinned fibers predominates (Fig. 2A). At higher $[Ca^{2+}]_O$ or during inotropic stimulation, peak intracellular $[Ca^{2+}]$ may reach levels closer to the flat portion of the Ca-force relationship in I79N mice, and little additional force is produced. Under those conditions, the impaired relaxation due to the increased myofibrillar Ca^{2+} -sensitivity predominates. Thus, the measured cardiac performance depends critically on the inotropic state of the preparation, and may differ depending on the experimental conditions.

What other factors besides the level of free Ca^{2+} could have contributed to the difference in systolic function measured under baseline conditions; i.e. increased *in vivo*, but no difference in the isolated heart? One explanation is that end-diastolic pressure was set at 8 mmHg for the isolated heart measurements. This experimental strategy allows one to compare contractile performance of hearts of different sizes, but underestimates developed pressure when diastolic compliance is impaired [Stromer, 1997 #14]. However, the lower LV balloon volume of I79N hearts would also be consistent with a decreased diastolic compliance. Thus, if diastolic compliance was impaired in the I79N hearts at a perfusate $[Ca^{2+}]_O$ of 2 mM, their systolic performance may actually have been underestimated in our isolated heart experiments.

Contractile indices obtained by echocardiography are significantly influenced by changes in preload and afterload. There are several reasons to believe that the reported *in vivo* results represent true differences in myocardial systolic performance: Afterload, as estimated by systolic blood

pressure, was not significantly different between Tg-I79N and Tg-WT. Although we did not directly measure the end-diastolic pressure (preload) *in vivo*, the end-diastolic LV dimensions can be used as a correlate, if heart rate and diastolic compliance are the same. End-diastolic LV dimensions were significantly smaller in the Tg-I79N mice, suggesting that either EDP was lower, or compliance was decreased in Tg-I79N mice. Thus, changes in preload are unlikely the explanation for the profound increase of the shortening fraction in the I79N mice.

In the Tg-I79N mice, ventricular relaxation was predicted to be slowed under basal conditions, based on our simulation studies, and at a $[Ca^{2+}]_o$ of 2 mM or above based on the isolated heart studies (table 1). Yet, we did not find evidence for impaired filling on Doppler under baseline conditions. One possibility is that the Doppler technique is not sensitive enough to detect subtle increases in diastolic chamber stiffness. Another possible explanation is the relatively low free $[Ca^{2+}]_o$ (1.25 mM) in mouse blood. In the isolated heart experiments, diastolic relaxation times were not significantly different at $[Ca^{2+}]_o$ of 0.5 or 1 mM, and EDP was significantly higher in the Tg-WT compared with Tg-I79N hearts (Fig. 2B). This increase of EDP at low $[Ca^{2+}]_o$ is somewhat surprising, but has been observed previously in the isolated heart preparation and is thought to be related to the turgor effect, when the perfusion pressure exceeds the systolic pressure during continuous retrograde perfusion (18).

Cardiac Electrophysiology and Arrhythmias

Unlike in the MHC403^{-/-} mouse model (23), ventricular arrhythmias were not observed in sedentary or exercised I79N mice at baseline. However, this may not be expected during the short period of ECG recordings employed in our study, since even in FHC patients ventricular arrhythmias are relatively rare, and occur on average less than 1 per month (6).

Surprisingly, transgenic mice expressing TnT-I79N had a consistently prolonged PR interval on ECG recordings. The PR prolongation was independent of the anesthetic used, was correlated to gene-dosage (Fig. 4C), and was more pronounced in chronically exercised (Fig. 4B). The duration of the PR interval is determined by conduction from the atria to the ventricle, and is controlled by the autonomic nervous system. An increase in vagal tone therefore could account for the PR prolongation, and could represent a reflex mechanism to increased cardiac contractility of I79N mice (e.g., via the baroreceptor reflex). The slower heart rate of conscious I79N mice is consistent with this hypothesis. Alternatively, atrial hypertrophy has been associated with PR prolongation in other mouse models of cardiac hypertrophy (10). We found significant atrial hypertrophy in I79N mice, and this may have contributed to the PR prolongation. The atrial hypertrophy could result from atrial I79N overexpression driven by the MHC promoter, which occurs earlier in the atria than in the ventricle (24), or might be a compensatory response to impaired diastolic relaxation of the ventricle, or both. Atrial hypertrophy has also been described in mice expressing the TnT-R92Q mutation (17).

Isoproterenol-induced contractile abnormalities, ECG Changes and Mortality

Based on our echocardiography and Doppler measurements, isoproterenol had little effect on systolic indices, but resulted in significantly altered measurements of diastolic filling in Tg-I79N mice. Although other factors such as pulmonary vein flow, end-diastolic pressure and atrial compliance can contribute to the shape of Doppler signals during mitral inflow, Doppler indices can be used to detect diastolic dysfunction: Little et. al. have shown that in particular the E-wave deceleration time is well correlated with diastolic chamber stiffness independently of preload (25). Accordingly, changes in this parameter could detect even the transient increase of diastolic chamber stiffness that occurs after coronary artery bypass surgery (26,27). Together with the data from the

isolated heart and the modeling studies, the significantly shortened E-wave deceleration time (table 2 and Fig. 5) in both transgenic lines suggests that isoproterenol induced an increased diastolic chamber stiffness in Tg-I79N mice. Obviously, an extensive cardiac catheterization study will have to confirm these observations in the future.

One surprising finding was the high mortality of Tg-I79N mice following the isoproterenol injection. Based on our Echocardiography and Doppler findings, the deaths were not caused by an aortic outflow obstruction, which is a common cause of death in end-stage human FHC (28). Deaths were also not due to ventricular tachyarrhythmias, another major cause of death in FHC patients (6), or hemorrhage. Rather, Tg-I79N mice died after isoproterenol induced changes in ECG morphology (loss of R-wave, ST segment depression and T-wave inversion) and heart block (Fig. 6). Although not diagnostic, similar ECG abnormalities can be observed with acute cardiac ischemia. Myocardial ischemia could be detected in all FHC patients that survived a cardiac arrest (29), and could play a role in the isoproterenol-induced mortality of Tg-I79N mice.

Several lines of evidence suggest that autonomic dysregulation could have contributed to the isoproterenol induced mortality: (i) Tg-I79N have evidence for increased in vagal output (lower basal heart rate, PR prolongation). (ii) Deaths occurred due to bradycardia and heart block. (iii) Isoproterenol-challenge can be used to induce vasovagal syncope in humans. (iv) In FHC patients, autonomic dysfunction can cause an inappropriate decrease in systemic vascular resistance at high work loads (30), and has been reported in a patient carrying a TnT mutation (4). Somewhat against this hypothesis speaks the fact that both ECG changes and Doppler abnormalities occurred before significant bradycardia was present. Thus, vagally-mediated bradycardia and vasodilation could have contributed to the Tg-I79N phenotype, but are likely not the sole explanation of the isoproterenol-induced mortality.

It remains to be determined why excess mortality was restricted to the isoproterenol challenge under anesthesia, and did not occur during the chronic swimming exercise, which should have produced a considerable endogenous catecholamine response. This suggests that the additional cardiovascular stress of anesthesia was needed to decompensate the Tg-I79N mice. On the other hand, sudden death in response to exercise is a rare event even in patients with FHC, and our chronic swimming exercise of 4 weeks in a limited number of mice might not have been sensitive enough to demonstrate significant differences in a rare event.

Thus, in an attempt to relate our previously published results obtained from skinned fibers to the data presented here, we suggest the following potential mechanisms for the isoproterenol-induced mortality: (i) The increased Ca^{2+} sensitivity of myofilaments (7) will enhance basal cardiac contractility (Table 2, Figs. 2 and 3), but the resulting slower decay of the Ca^{2+} -transient and force could prevent or hinder the increase in relaxation rate which normally occurs after β -adrenergic stimulation, causing diastolic dysfunction (Figs. 2 and 5) (ii) The loss of the protective myofilamental pH-regulation (*e.g.*, the loss of contractile uncoupling at low pH previously reported (7)), could worsen any regional oxygen supply-demand mismatch induced by impaired diastolic relaxation (Fig. 1). Thus, the isoproterenol-induced ECG changes (Fig. 7) may represent evidence for regional myocardial ischemia or direct catecholamine toxicity. (iii) Although I79N fibers may produce more force at low $[\text{Ca}^{2+}]_o$ (Fig. 2A), raising $[\text{Ca}^{2+}]$ provides little increase in force, since the fibers are already operating close to the flat part of the force/pCa relationship. Thus, the lower maximal force per cross-sectional area previously reported (7) might decrease the contractile reserve available to increase cardiac output appropriately in response to isoproterenol-induced vasodilatation. (iv) The cardiac hypercontractility may activate ventricular mechanoreceptors and thereby cause chronic alterations in vagal tone, which could contribute to bradycardia and death in

response to isoproterenol. In summary, Tg-I79N mice may become a valuable model to explore potential mechanisms of sudden death induced by the TnT-I79N mutation.

Acknowledgments

We are very grateful for the help of Dr. Carl Apstein, who taught us the technique of isovolumic contractility measurements in the isolated mouse heart.

References

1. Watkins, H., McKenna, W. J., Thierfelder, L., Suk, H. J., Anan, R., O'Donoghue, A., Spirito, P., Matsumori, A., Moravec, C. S., Seidman, J. G., and et al. (1995) *N Engl J Med* **332**(16), 1058-64
2. Watkins, H., Seidman, C. E., Seidman, J. G., Feng, H. S., and Sweeney, H. L. (1996) *J Clin Invest* **98**(11), 2456-61
3. Moolman, J. C., Corfield, V. A., Posen, B., Ngumbela, K., Seidman, C., Brink, P. A., and Watkins, H. (1997) *J Am Coll Cardiol* **29**(3), 549-55
4. Varnava, A., Baboonian, C., Davison, F., de Cruz, L., Elliott, P. M., Davies, M. J., and McKenna, W. J. (1999) *Heart* **82**(5), 621-4
5. Ho, C. Y., Lever, H. M., DeSanctis, R., Farver, C. F., Seidman, J. G., and Seidman, C. E. (2000) *Circulation* **102**(16), 1950-5
6. Maron, B. J., Shen, W. K., Link, M. S., Epstein, A. E., Almquist, A. K., Daubert, J. P., Bardy, G. H., Favale, S., Rea, R. F., Boriani, G., Estes, N. A., 3rd, and Spirito, P. (2000) *N Engl J Med* **342**(6), 365-73
7. Miller, T., Szczesna, D., Housmans, P. R., Zhao, J., deFreitas, F., Gomes, A. V., Culbreath, L., McCue, J., Wang, Y., Xu, Y., Kerrick, W. G., and Potter, J. D. (2000) *J Biol Chem* **in press**
8. Lim, C. C., Liao, R., Varma, N., and Apstein, C. S. (1999) *Am J Physiol* **277**(5 Pt 2), H2083-90
9. Fabiato, A. (1988) *Methods Enzymol* **157**, 378-417
10. Knollmann, B. C., Knollmann-Ritschel, B. E. C., Weissman, N. J., Jones, L. R., and Morad, M. (2000) *J Physiol* **525** (part2), 483-498

11. Mitchell, G. F., Jeron, A., and Koren, G. (1998) *Am J Physiol* **274**(3 Pt 2), H747-51
12. Hoit, B. D., Khoury, S. F., Kranias, E. G., Ball, N., and Walsh, R. A. (1995) *Circ Res* **77**(3), 632-7
13. Geisterfer-Lowrance, A. A., Christe, M., Conner, D. A., Ingwall, J. S., Schoen, F. J., Seidman, C. E., and Seidman, J. G. (1996) *Science* **272**(5262), 731-4
14. Robertson, S. P., Johnson, J. D., and Potter, J. D. (1981) *Biophys J* **34**(3), 559-69
15. Mikane, T., Araki, J., Kohno, K., Nakayama, Y., Suzuki, S., Shimizu, J., Matsubara, H., Hirakawa, M., Takaki, M., and Suga, H. (1997) *Am J Physiol* **273**(6 Pt 2), H2891-8
16. Landesberg, A., and Sideman, S. (1999) *Am J Physiol* **276**(3 Pt 2), H998-H1011
17. Tardiff, J. C., Hewett, T. E., Palmer, B. M., Olsson, C., Factor, S. M., Moore, R. L., Robbins, J., and Leinwand, L. A. (1999) *J Clin Invest* **104**(4), 469-81
18. Spindler, M., Saupe, K. W., Christe, M. E., Sweeney, H. L., Seidman, C. E., Seidman, J. G., and Ingwall, J. S. (1998) *J Clin Invest* **101**(8), 1775-83
19. Georgakopoulos, D., Christe, M. E., Giewat, M., Seidman, C. M., Seidman, J. G., and Kass, D. A. (1999) *Nat Med* **5**(3), 327-30
20. Apstein, C. S., Deckelbaum, L., Hagopian, L., and Hood, W. B., Jr. (1978) *Am J Physiol* **235**(6), H637-48
21. Christensen, G., Wang, Y., and Chien, K. R. (1997) *Am J Physiol* **272**(6 Pt 2), H2513-24
22. Lim, D. S., Oberst, L., McCluggage, M., Youker, K., Lacy, J., DeMayo, F., Entman, M. L., Roberts, R., Michael, L. H., and Marian, A. J. (2000) *J Mol Cell Cardiol* **32**(3), 365-74
23. Berul, C. I., Christe, M. E., Aronovitz, M. J., Seidman, C. E., Seidman, J. G., and Mendelsohn, M. E. (1997) *J Clin Invest* **99**(4), 570-6
24. Subramaniam, A., Jones, W. K., Gulick, J., Wert, S., Neumann, J., and Robbins, J. (1991)

J Biol Chem **266**(36), 24613-20

25. Little, W. C., Ohno, M., Kitzman, D. W., Thomas, J. D., and Cheng, C. P. (1995) *Circulation* **92**(7), 1933-9
26. McKenney, P. A., Apstein, C. S., Mendes, L. A., Connelly, G. P., Aldea, G. S., Shemin, R. J., and Davidoff, R. (1999) *Am J Cardiol* **84**(8), 914-8
27. McKenney, P. A., Apstein, C. S., Mendes, L. A., Connelly, G. P., Aldea, G. S., Shemin, R. J., and Davidoff, R. (1994) *J Am Coll Cardiol* **24**(5), 1189-94
28. Wigle, E. D., Rakowski, H., Kimball, B. P., and Williams, W. G. (1995) *Circulation* **92**(7), 1680-92
29. Dilsizian, V., Bonow, R. O., Epstein, S. E., and Fananapazir, L. (1993) *J Am Coll Cardiol* **22**(3), 796-804
30. Prasad, K., and Frenneaux, M. P. (1998) *Heart* **79**(6), 538-40

Legends

Figure 1 Left-ventricular isovolumic pressure tracings from Tg-WT and Tg-I79N (line 9) mice

Representative examples of isovolumic pressure tracings recorded at 1kHz from a Tg-WT and a Tg-I79N heart. Note the faster onset of pressure rise (arrow) and the slower pressure decay in the Tg-I79N heart.

Figure 2 Relationship between Ca^{2+} concentration and isovolumic contractile performance

A: Developed pressure, **B:** End-diastolic pressure (EDP), and **C:** Time to 90% relaxation as a function of perfusate Ca^{2+} concentrations in hearts from Tg-I79N mice (line 9, filled squares) and from Tg-WT mice (open squares). Data are expressed as means \pm SEM, * $p < 0.05$.

Figure 3 Echocardiography and Doppler measurements from Tg-WT and Tg-I79N (line 9) mice.

A: Representative examples of 2D-guided M-mode recordings obtained with a high-resolution 13 MHz transducer. Tg-I79N mice demonstrate an increased left-ventricular (LV) shortening fraction at baseline. LVD: LV diastolic diameter, LVS: LV systolic diameter.

B: Representative examples of 2D-guided Doppler recordings of aortic outflow velocity. Tg-I79N mice demonstrate a shorter acceleration time (=time from opening of the aortic valve to peak flow velocity) at baseline.

Figure 4 ECG recordings from non-Tg, Tg-WT and Tg-I79N (line 9) mice.

A: Representative ECG tracings (lead I). The various ECG parameters are indicated: P represents atrial contraction (P-wave), QRS the ventricular depolarization (QRS complex), and T the ventricular repolarization (T-wave). A longer PR interval (=atrioventricular conduction) and a shorter QT interval (=ventricular repolarization) were consistently encountered in Tg-I79N vs. Tg-WT and non-Tg mice.

B: Effect of chronic exercise on the PR interval. Chronic swimming exercise (4 weeks) resulted in a significantly longer PR interval only in Tg-I79N mice.

C: Effect of protein expression levels on the PR interval. I79N mice expressing higher protein levels of the mutant Tnt-I79N (line 8) had a significantly longer PR interval compared with mice expressing lower protein levels of mutant TnT-I79N (line 9).

Figure 5 Mitral inflow velocity measurements after low-dose isoproterenol.

Representative examples of 2D-guided Doppler recordings of mitral inflow velocity after low-dose isoproterenol (0.1 mg/kg i.p.). I79N mice have a faster deceleration of the E-wave (= early diastolic mitral inflow velocity) and decreased A-wave amplitude (=late diastolic mitral inflow velocity due to atrial contraction). These findings are consistent with increased diastolic ventricular chamber stiffness.

Figure 6 Dose-dependence of isoproterenol-induced ECG changes and mortality.

ECG changes (loss of R-wave amplitude, QRS widening, T-wave inversion) and mortality were quantified at a low dose (0.1 mg/kg i.p., panel A) and a high dose (1.5 mg/kg i.p., panel B) of isoproterenol by intraperitoneal injection. The effect of isoproterenol on ECG and mortality was dose-dependent.

Figure 7 Heart rate response and ECG changes after isoproterenol.

Representative heart rate response and ECG morphology after intraperitoneal (i.p.) injection of isoproterenol (1.5 mg/kg). The insets illustrate the changes in ECG morphology over time. Compared to Tg-WT mice (upper panel), Tg-I79N mice (lower panel) develop a rapid increase, followed by a

progressive decrease in heart rate, which is accompanied by characteristic changes in ECG morphology (loss of R-wave, QRS widening and T-wave inversion, inset D). Tg-I79N mice then die from progressive conduction blocks (PR prolongation, and 2nd and 3rd degree atrioventricular block (AVB), insets E, F and G).

Figure 8 Histological examination

Hematoxylin and eosin (H+E) (upper panels) and trichrome (TRIC) (lower panels) stained ventricular sections from Non-Tg, Tg-WT (line 3) and Tg-I79N (line 9). Note normal myocyte architecture and no major differences between the three lines.

Table 1 Baseline contractile parameters in the isovolumetrically contracting mouse hearts (mean \pm SEM)

	Non-Tg n=4	Tg-WT n=5	Tg-I79N (line 9) n=5
End-diastolic pressure (mmHg)	8.4 \pm 0.5	7.6 \pm 0.5	7.7 \pm 0.3
Systolic pressure (mmHg)	76 \pm 6.7	70 \pm 5.7	71 \pm 6.1
Developed pressure (mmHg)	68 \pm 6.3	62 \pm 5.3	63 \pm 6.0
Peak +dP/dt (mmHg/s)	3517 \pm 292	2973 \pm 222	3140 \pm 302
Time to peak pressure (ms)	39 \pm 0.5	40 \pm 1.3	40 \pm 0.3
Time to peak +dP/dt (ms)	12.5 \pm 0.4	12.4 \pm 0.2	10.6 \pm 0.3**
Peak -dP/dt (mmHg/s)	2587 \pm 305	2163 \pm 193	1867 \pm 212
Ratio (+dP/dt to -dP/dt)	1.38 \pm 0.08	1.39 \pm 0.06	1.69 \pm 0.07*
Time to 90% relaxation (ms)	38 \pm 1.0	41 \pm 0.4	49 \pm 1.5***
Tau (ms)	15 \pm 0.8	16 \pm 0.8	21 \pm 0.4***

*p<0.05, **p<0.01, ***p<0.001, Tg-I79N vs. non-Tg or Tg-WT; Oneway ANOVA followed by unpaired Student's *t*-test

Table 2 Echocardiography and Doppler measurements under Avertin and Ketamine/Xylazine anesthesia (mean \pm SEM)

	Baseline (Ketamine/Xylazine)				Baseline (Avertin)			Isoproterenol (Ketamine/Xylazine)			
	Non-Tg	Tg-WT	Tg-I79N (line 9)	Tg-I79N (line 8)	Non-Tg	Tg-WT	Tg-I79N (line 9)	Non-Tg	Tg-WT	Tg-I79N (line 9)	Tg-I79N (line 8)
	n=7	n=11	n=7	n=6	n=34	n=26	n=37	n=7	n=12	n=7	n=6
HR (b/min)	223 \pm 23	233 \pm 15	206 \pm 25	275 \pm 1	464 \pm 9	451 \pm 10	442 \pm 10	474 \pm 39	480 \pm 26	481 \pm 40	494 \pm 26
Septum (mm)	.7 \pm .03	.8 \pm .03	.8 \pm .03	.7 \pm .05	.65 \pm .02	.69 \pm .02	.61 \pm .01**	.8 \pm .05	.7 \pm .04	.7 \pm .03	.6 \pm .06
LVEDD (mm)	3.6 \pm .1*	4.2 \pm .2	4.0 \pm .2	3.3 \pm .1**	3.6 \pm .07	3.8 \pm .09	3.2 \pm .07**	3.0 \pm .2	3.3 \pm .1	3.4 \pm .1	2.9 \pm .1
LVESD (mm)	2.1 \pm .2	2.7 \pm .2	2.1 \pm .3	1.8 \pm .2*	2.4 \pm .08*	2.8 \pm .10	1.9 \pm .07**	1.2 \pm .07	1.2 \pm .1	1.5 \pm .1	1.3 \pm .2
LVPW(mm)	.8 \pm .04	.7 \pm .03	.8 \pm .03	.8 \pm .03	.63 \pm .01	.63 \pm .01	.61 \pm .01	.7 \pm .06	.8 \pm .03	.8 \pm .03	.7 \pm .03
LVSF (%)	41 \pm 5	35 \pm 3	48 \pm 4**	47 \pm 5*	33 \pm 1**	27 \pm 1	43 \pm 2**	59 \pm 4	62 \pm 3	57 \pm 3	55 \pm 6
VCFc (circ/s)	3.0 \pm .4	2.4 \pm .2	3.6 \pm .4**	3.0 \pm .2*	1.5 \pm .1*	1.1 \pm .1	2.1 \pm .1**	4.3 \pm 0.4	4.1 \pm .2	3.5 \pm .2	3.5 \pm .5
LVOT (cm/s)	60 \pm 4	63 \pm 2	74 \pm 5*	50 \pm 5*	60 \pm 2**	51 \pm 2	60 \pm 2**	95 \pm 4	98 \pm 5	95 \pm 5	71 \pm 5**
ET (ms)	75 \pm 6	78 \pm 2	77 \pm 6	73 \pm 4	67 \pm 1	71 \pm 2	72 \pm 1	51 \pm 3	56 \pm 2	58 \pm 2	56 \pm 1
AT (ms)	17 \pm 1**	23 \pm 1	17 \pm 2**	18 \pm 1*	21 \pm .8	22 \pm .8	20 \pm .7*	17 \pm 2	16 \pm 1	17 \pm 1	14 \pm 1
E-wave (cm/s)	63 \pm 7	61 \pm 4	62 \pm 6	57 \pm 4	52 \pm 3	47 \pm 3	43 \pm 2	77 \pm 3	76 \pm 3	73 \pm 3	60 \pm 4**
A-wave (cm/s)	22 \pm 4	24 \pm 3	16 \pm 3	21 \pm 5	43 \pm 2	44 \pm 5	33 \pm 4	69 \pm 6	69 \pm 4	26 \pm 4**	43 \pm 10*
DT (ms)	32 \pm 4	34 \pm 3	32 \pm 3	33 \pm 4	32 \pm 2	34 \pm 4	34 \pm 2	42 \pm 5	42 \pm 3	23 \pm 3**	31 \pm 4*
E:A ratio ^{&}	3.3 \pm .4	3.1 \pm .4	4.5 \pm .9	3.9 \pm 1.1	1.3 \pm .1	.9 \pm .2	1.5 \pm .2	1.1 \pm .1	1.0 \pm .1	4.2 \pm .1*	1.8 \pm .7

HR: heart rate, LV: Left ventricle, LVEDD: LV end-diastolic dimension, LVESD: LV end-systolic dimension, LVSF: LV shortening fraction, VCFc: Heart-rate corrected velocity of circumferential fiber shortening, LVOT: LV peak outflow velocity, ET: Aortic ejection time, AT: Aortic acceleration time, DT: E-wave deceleration time. A-wave, DT and E:A ratio could only be measured in <30% of mice under Avertin anesthesia.

* p<0.05 vs. Tg-WT, **p<0.01 vs. Tg-WT, Oneway ANOVA followed by unpaired Student's *t*-test; [&]median values are reported for isoproterenol data.

Figure 1

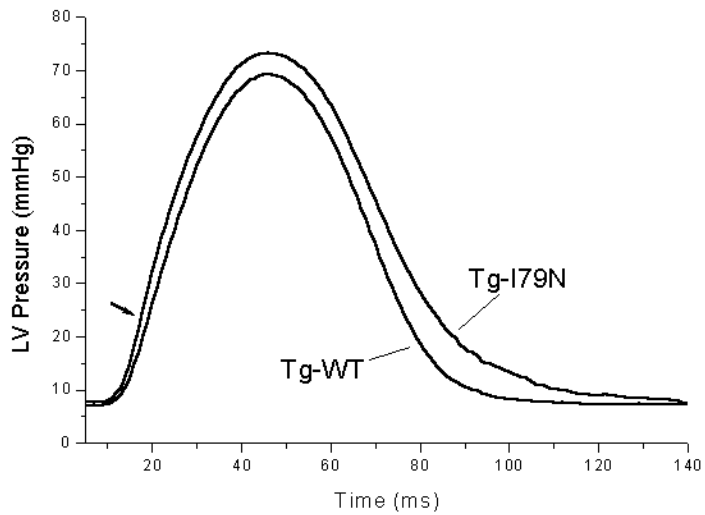


Figure 2A

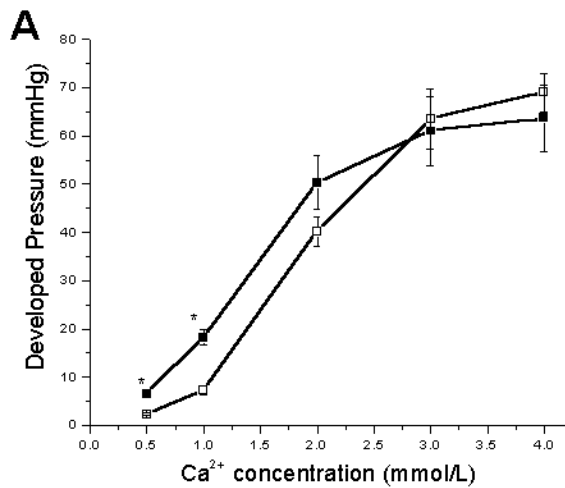


Figure 2B

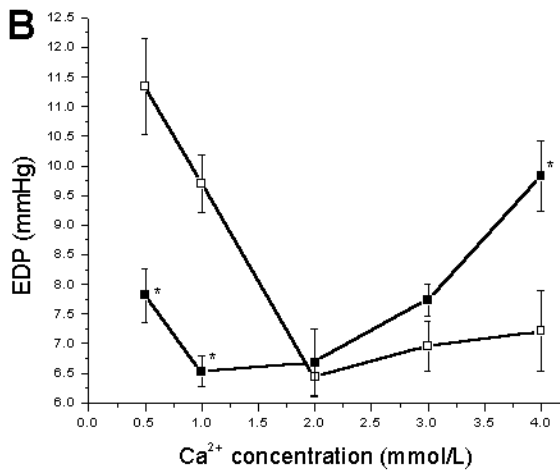


Figure 2C

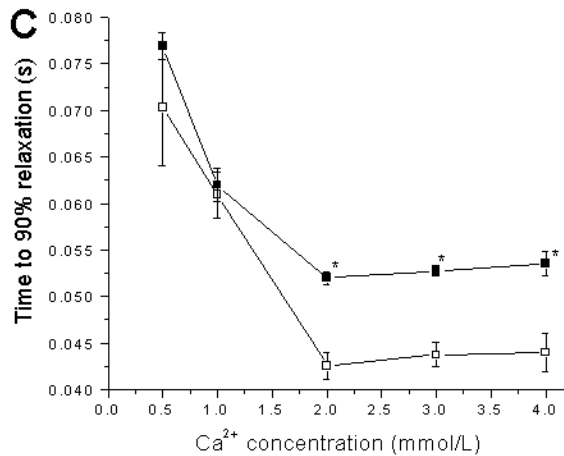


Figure 3

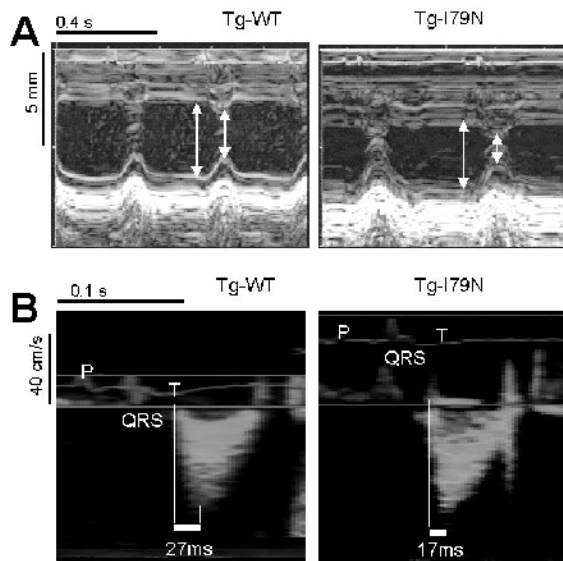


Figure 4

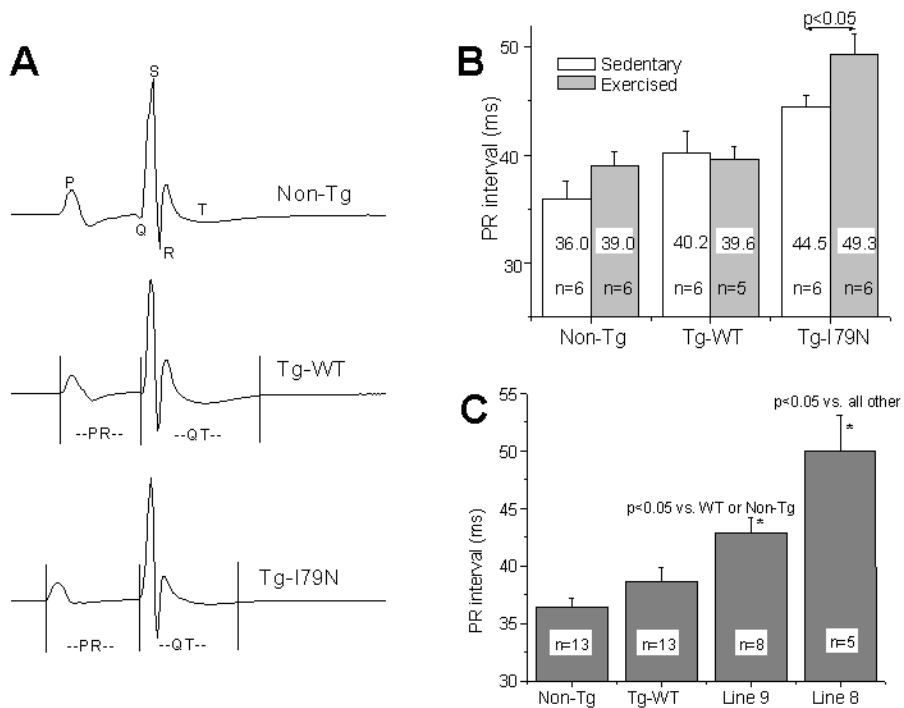


Figure 5

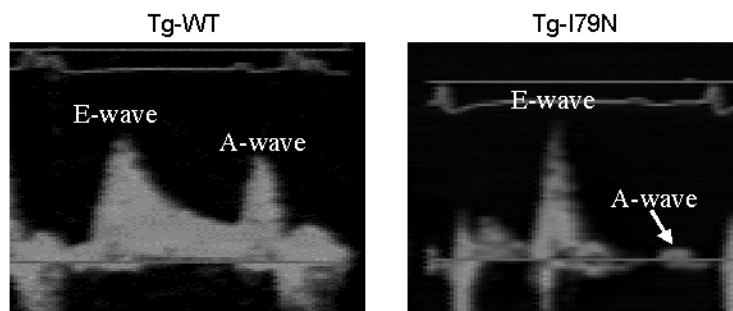


Figure 6

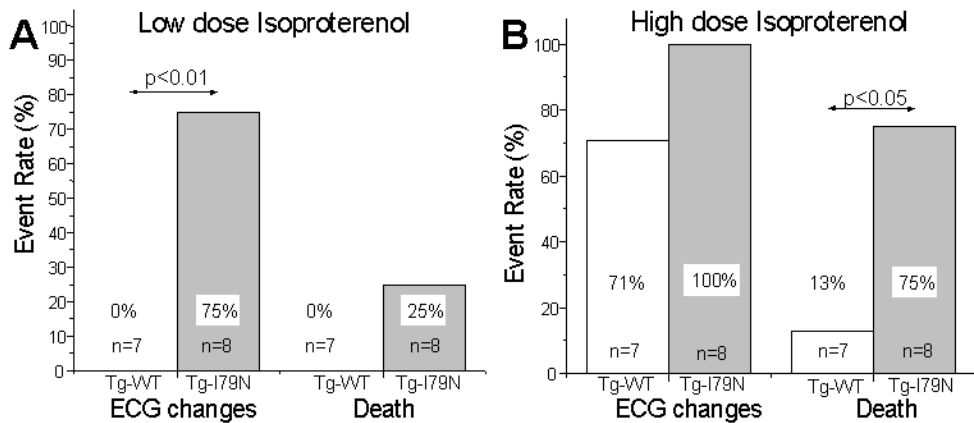


Figure 7 upper panel

Tg-WT

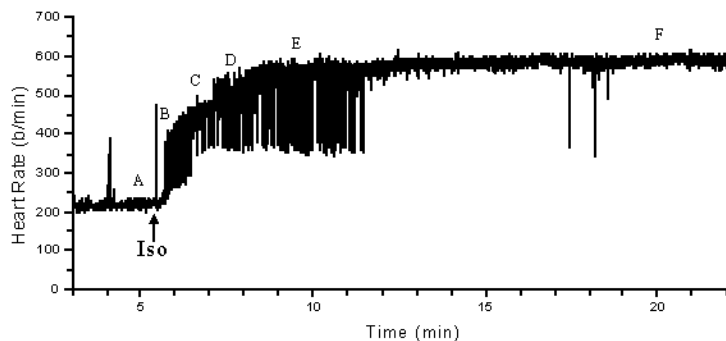
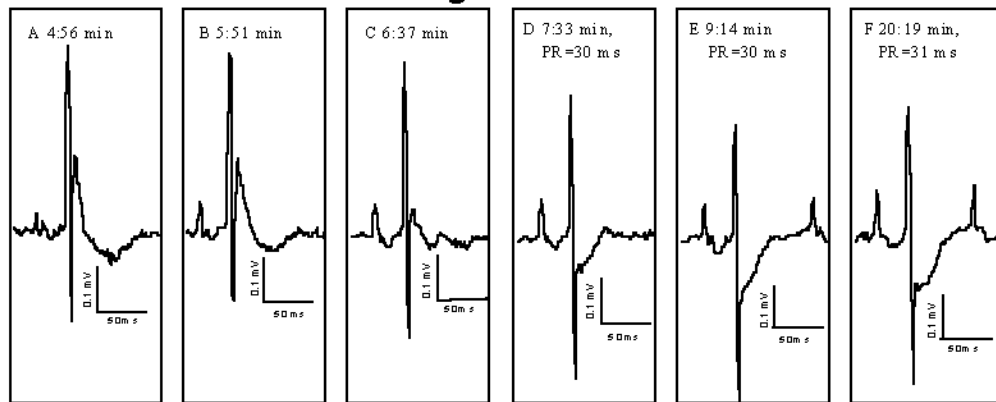


Figure 7 lower panel

Tg-I79N

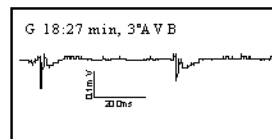
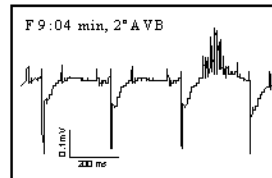
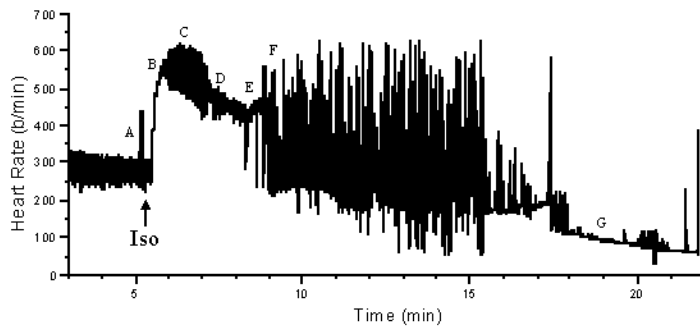
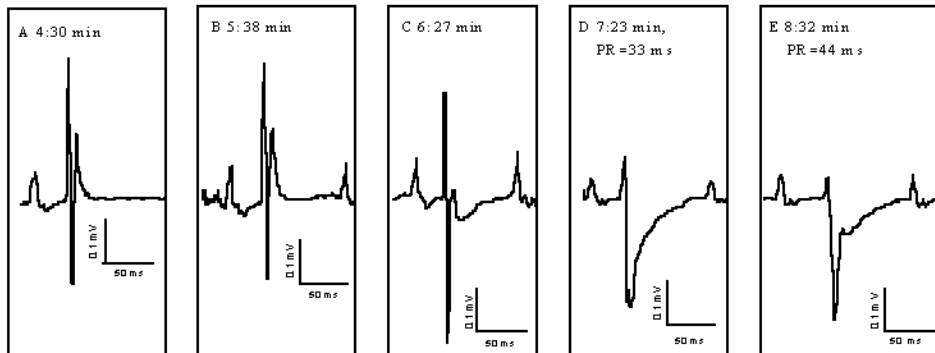
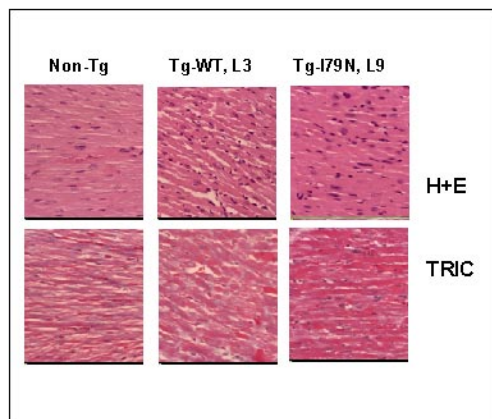


Figure 8



**INOTROPIC STIMULATION INDUCES CARDIAC DYSFUNCTION IN
TRANSGENIC MICE EXPRESSING A TROPONIN T (I79N) MUTATION LINKED
TO FAMILIAL HYPERTROPHIC CARDIOMYOPATHY**

Bjorn C. Knollmann, Stephen A. Blatt, Kenneth Horton, Fatima de Freitas, Todd E. Miller,
Michael Bell, Philippe R. Housmans, Neil J. Weissman, Martin Morad and James D. Potter

J. Biol. Chem. published online December 11, 2000

Access the most updated version of this article at doi: [10.1074/jbc.M006745200](https://doi.org/10.1074/jbc.M006745200)

Alerts:

- [When this article is cited](#)
- [When a correction for this article is posted](#)

[Click here](#) to choose from all of JBC's e-mail alerts